Maternal Exposure to Sevoflurane Disrupts Oligodendrocyte Myelination of the Postnatal Hippocampus and Induces Cognitive and Motor Impairments in Offspring

Ze Fan
Fourth Military Medical University School of Stomatology: Air Force Medical University School of Stomatology

Lirong Liang
Fourth Military Medical University School of Stomatology: Air Force Medical University School of Stomatology

Ruixue Ma
Fourth Military Medical University: Air Force Medical University

Rougang Xie
Fourth Military Medical University: Air Force Medical University

Youyi Zhao
Fourth Military Medical University School of Stomatology: Air Force Medical University School of Stomatology

Ming Zhang
Fourth Military Medical University: Air Force Medical University

Baolin Guo
Fourth Military Medical University: Air Force Medical University

Tian Zeng
Fourth Military Medical University School of Stomatology: Air Force Medical University School of Stomatology

Danyi He
Fourth Military Medical University School of Stomatology: Air Force Medical University School of Stomatology

Xianghui Zhao
Fourth Military Medical University: Air Force Medical University

Hui Zhang (✉ zhanghuifmmua@163.com)
Fourth Military Medical University School of Stomatology: Air Force Medical University School of Stomatology https://orcid.org/0000-0003-1183-787X

Research Article

Keywords: Sevoflurane, Neurotoxicity, Oligodendrocyte, Myelination, Hippocampus, Cognition

Posted Date: August 23rd, 2021

DOI: https://doi.org/10.21203/rs.3.rs-763902/v1

Abstract

Maternal exposure to sevoflurane can impose significant neurocognitive risks on the developing brain of infants. Several studies have indicated that oligodendrocytes may be involved in sevoflurane-induced neurotoxicity, but the concrete effects of sevoflurane on the development and myelination of oligodendrocytes remain unclear. In this study, we assessed fetal myelination and neural behavior after maternal exposure to sevoflurane. Pregnant C57BL/6J mice (gestational day 15.5) were exposed to sevoflurane (2.5%) for 6 h. The cognitive function and motor coordination of offspring (8 weeks of age) were determined via the novel object recognition test, the Morris water maze test and the accelerating rotarod test. Proliferation and differentiation of cultured oligodendrocyte precursor cells (OPCs) were detected via immunocytochemistry. Expression and ultrastructure of myelin in the fetal hippocampus were analyzed using immunohistochemistry and transmission electron microscopy (TEM). Myelin-associated genes and proteins were tested via qRT-PCR, immunofluorescence and western blotting. The functionality of myelin was evaluated by electrophysiology. The results showed that maternal exposure to sevoflurane induced cognitive and motor impairments in infants, accompanied by inhibitions of OPC proliferation and differentiation, and damages of myelin structure. Myelin-associated genes and proteins (including MBP, Olig1, PDNFRα, Sox10, etc.) were downregulated. The conduction velocity of axons also declined. These results suggested that maternal exposure to sevoflurane could induce detrimental effects on cognitive and motor functions in offspring, which might be associated with disrupted myelination of oligodendrocytes in the hippocampus.

Introduction

Advances in surgical technologies have led to a substantial increase in the number of pregnant women undergoing general anesthesia (Wang et al. 2018). Subsequently, there has been increasing concerns regarding the safety of maternal anesthesia for offspring (Chai et al. 2019). Mounting and convincing preclinical evidences in rodents and nonhuman primates indicate that exposure to anesthetic agents during the mid-trimester period may induce widespread neuronal cell death (Perez-Zoghbi et al. 2017; Xu et al. 2018) and long-term behavioral abnormalities in offspring (Wu et al. 2018), such as deficiency in learning and memory (Dong et al. 2016; Makaryus et al. 2015). Therefore, the Food and Drug Administration (FDA) in the United States issued a “Drug Safety Communication” warning that “repeated or lengthy use of general anesthetics or sedation drugs during surgeries or procedures in children younger than 3 years old or in pregnant woman during the third trimester may affect the development of children’s brains” (Andropoulos et al. 2017).

Sevoflurane is one of the most commonly used inhalation anesthetic agents in obstetric and pediatric surgeries (Lee et al. 2017). Due to its lipophilicity, sevoflurane can easily cross the placenta and blood-brain barrier, and affect the development of the brain of infants (Fang et al. 2017). Several mechanisms have been proposed to be involved in sevoflurane-induced neurotoxicity, including apoptosis, inflammation, disruption of synaptogenesis and so on (Neag et al. 2020). However, most of these mechanisms are focused on neurons, not glial cells (Zheng et al. 2013). Given the integrity of the central

nervous system (CNS) and the crucial role of oligodendrocytes in the development and functional maintenance of neurons (Xin et al. 2020), the potential effects of sevoflurane exposure on oligodendrocytes should not be neglected.

In the developing CNS, oligodendrocytes extend membrane processes by ensheathing neuronal axons with lipid-rich myelin membranes. Myelination enables axons to transmit information more rapidly, which facilitates the evolution of a complex yet compact CNS in vertebrate animals (Elbaz et al. 2019). In addition, myelin plays a critical role in proper neuronal function by providing trophic and metabolic support to axons and facilitating energy-efficient saltatory conduction (Ishii et al. 2019). Impairment of oligodendrocyte myelination has been shown to be associated with many neurological diseases, including autism, Alzheimer's disease and depression (Lu et al. 2016). However, whether exposure to sevoflurane during the gestational period influences the myelination and development of oligodendrocytes is still elusive.

In this study, we evaluated the effects of maternal exposure to sevoflurane on myelination in the hippocampus and the long-term cognition and motor performance of postnatal mice. Our results demonstrated that sevoflurane exposure during the prenatal period induced impairments in the structure of myelin, as well as deficits in long-term memory and fine motion. In addition, we observed inhibitions of proliferation and differentiation of oligodendrocyte precursor cells (OPCs), and reduction of the expression of RNAs and proteins involved in the regulation of oligodendrocyte development. The function of axonal conduction velocity was also attenuated. Altogether, these results suggested that early gestational exposure to sevoflurane could induce detrimental effects on cognitive and motor functions of postnatal mice, which might be associated with disrupted oligodendrocyte myelination in the hippocampus.

Materials And Methods

Animals and Experimental Design

All procedures of the study were approved by the Animal Care and Use Committee of the Fourth Military Medical University (Xi'an, China) and followed institutional guidelines. C57BL/6J male and female mice (8-week-old) were provided by the Animal Centre of the Fourth Military Medical University. Pairs of female mice mated with one male, and pregnant mice were identified and placed into another cage. All mice were housed and allowed free access to a standard animal diet and tap water. Room temperature was maintained at 20~23 °C with a 12 h/12 h light/dark cycle.

A total of 108 offspring mice (6 per group in functional tests and 4 per group in morphological tests) were used in this study on the basis of scientific literatures and our pre-test results. Briefly, morphological changes of oligodendrocytes were detected via immunofluorescence, western blot, PCR and electron microscope at PND14, PND30 and PND60 after maternal exposure to sevoflurane, while functional changes were detected via electrophysiological and behavioral tests at PND30 and PND60 (Fig. 1a). All

experiments were carried out in triplicate, and randomization and double-blinding were conducted to minimize subjective bias in the design.

Sevoflurane Exposure

Pregnant C57BL/6J mice were randomly assigned to the control group or the sevoflurane-treated group on gestational day 15.5 (G15.5). Mice in the sevoflurane-treated group received 2.5% sevoflurane in 97.5% oxygen for 6 h in an anesthetizing box, while mice in the control group received 100% oxygen for 6 h. The size of the anesthetizing box was 15 × 15 × 35 cm^3. The gas flow rate was 2 L/min for induction and 1 L/min for maintenance. The concentrations of sevoflurane and oxygen were continuously monitored with a gas analyzer (Drager, Germany). A warming blanket was used during anesthesia to prevent hypothermia.

OPC Culture and Sevoflurane Exposure

Primary OPCs were prepared from the hippocampus of postnatal day 1 (PND1) to PND2 pups. Briefly, cells were dissociated and maintained in Dulbecco's modified Eagle's medium (SH30022, HyClone, USA, 25 mM glucose) containing 10% fetal bovine serum (16140071, Thermo Fisher Scientific (TFS), USA) and 1% penicillin/streptomycin (15140122, Gibco, USA). After shaking at 200 rpm for 1 h to remove microglia, fresh medium was added and shaken overnight. The cells in the supernatant were plated and expanded in neurobasal medium (21103049, TFS) containing 1% glutamine (25030081, Gibco), 10 ng/ml PDGF (PHG0035, Gibco), 10 ng/ml bFGF (PHG0021, Gibco) and 2% B27 supplement (17054044, Gibco). Half of the culture medium was replaced with fresh OPC culture medium every 3 days to feed the cultured cells.

Cultured OPCs were treated with sevoflurane through a vaporizer (Abbott, USA). Cells were placed in an airtight incubation chamber (Billups-Rothenberg, USA) at 37 °C and subsequently perfused with air (21% O2, 5% CO2, 69% N2) containing 4.1% sevoflurane for 6 h. The gas concentrations of O2, CO2 and sevoflurane were continuously monitored by an anesthetic gas measurer module (Datex Ohmeda, Spain). The cells in the control group were perfused for the same time with fresh air. Once the exposure was finished, the cells were returned to the incubator.

Immunocytochemistry and BrdU Incorporation

For immunocytochemistry, cells were fixed with 4% paraformaldehyde for 10 min. For BrdU incorporation analysis, cells were treated with 2 N HCl after fixation for 10 min at 37 °C to denature DNA, followed by neutralization with borate buffer (0.1 M, pH 8.5) for 10 min at room temperature. After blocking with 3% BSA and 0.3% Triton X-100 in PBS for 30 min, cells were incubated with the following primary antibodies overnight at 4 °C: rabbit anti-BrdU (1:200, Abcam Cat# ab152095, RRID: AB_2813902) (Armistead et al.), mouse anti-Olig2 (1:200, TSF Cat# MA5-15810, RRID: AB_11152534) (Wong et al.), and rabbit anti-MBP (1:500, Abcam Cat# ab40390, RRID:AB_1141521) (Morrison et al. 2016). After 3 washes with PBS, cells were incubated with a mixture of AlexaFluor 488-conjugated donkey anti-rabbit (1:800, TFS Cat# A32790, RRID: AB_2762833) and 594-conjugated donkey anti-mouse (1:800, TFS Cat# A32744, RRID:

AB_2762826) secondary antibodies for 1 h at room temperature. Nuclei were stained with DAPI (4',6-diamidino-2-phenylindole, 1:1000, Sigma-Aldrich, USA). A confocal system (Olympus Fluoview Ver4.2b, Japan) was used for image acquisition. Briefly, slides were scanned under a laser confocal microscope with wavelengths at 405 nm, 488 nm and 543 nm. The parameters were setup as follows: Object lens (20 magnification); filter mode (Kalman and line 2); Sequential (Line); Pixel (1024by*1024by). All images were captured in a dark room at a temperature of 25℃. Image J software was used for image analysis.

Immunohistochemistry

Animals were deeply anesthetized with pentobarbital and transcardially perfused with PBS followed by 4% paraformaldehyde. Then, the brains were collected and postfixed for 2 h. After transfer to a gradient of sucrose (20% and 30% in PBS), 30 μm thin serial coronal sections encompassing the entire hippocampus were collected using a freezing microtome (Leica, Germany). The sections were kept in citrate buffer at 86 °C for 15 min for antigen retrieval, followed by blocking with 3% BSA and 0.3% Triton X-100 for 1 h. Next, the sections were incubated with the following primary antibodies overnight at 4 °C: rabbit anti-Olig2 (1:500, Abcam Cat# ab109186, RRID: AB_10861310) (Milosevic et al. 2017), rabbit anti-PDGFRα (1:500, Abcam Cat# ab203491, RRID: AB_2892065) (Du et al. 2020), rabbit anti-MBP (1:500, Abcam Cat# ab40390, RRID: AB_1141521) (Morrison et al. 2016), mouse anti-NF (1:500, GeneTex Cat# GTX27795, RRID: AB_366933) (Cortés-Medina et al. 2019), and mouse anti-CC1 (1:200, GeneTex Cat# GTX16794, RRID: AB_422404) (Göttle et al. 2015). After washing 3 times with PBS, the sections were incubated with an appropriate combination of AlexaFluor 488-conjugated donkey anti-rabbit (1:800, TFS Cat# A32790, RRID: AB_2762833) and 594-conjugated donkey anti-mouse (1:800, TFS Cat# A32744, RRID: AB_2762826) secondary antibodies for 2 h at room temperature. Nuclei were stained with DAPI (1:1000, Sigma-Aldrich), and fluorescence images were captured using a confocal system (Olympus Fluoview Ver4.2b, Japan) as mentioned above.

Quantitative real-time PCR

Total RNA from hippocampal tissue was extracted using TRIzol reagent (15596026, TSF). The quality and quantity of RNA were detected using a NanoDrop spectrophotometer (ND-NDL-2YRW-CCC, TSF). Equal amounts of RNA were reverse transcribed to cDNA by using a SuperScript first-strand cDNA synthesis kit (18080051, TSF) with Oligo-dT. qRT-PCR was performed with SYBR Green Master Mix (a46109, TSF) using the ABI Prism 7900 Sequence Detector System (PE Applied Biosystems, USA). Expression of GAPDH was served as control to normalize values. Relative RNA expression was calculated using the $2^{-\Delta\Delta Ct}$ method.

Western blotting

Tissues were lysed in lysis buffer (89901, TSF) containing inhibitors of protease and phosphatase (78442, TSF). Protein concentrations were estimated using a bicinchoninic acid (BCA) protein assay kit (23227, TSF). An equivalent amount of protein (30 μg) from each sample was resolved on SDS-polyacrylamide gels and then transferred to PVDF membranes (88520, TSF). Next, the membranes were

blocked in a 5% skimmed milk solution for 1 h at room temperature, followed by incubation overnight at 4 °C with the following rabbit primary antibodies: β-tubulin (1:1000, Abcam Cat# ab179513) (Li et al. 2019), Olig1 (1:1000, GeneTex Cat# GTX104823, RRID: AB_1241130), Olig2 (1:1000, Abcam Cat# ab109186, RRID: AB_10861310) (Milosevic et al. 2017), PDGFRα (1:1000, Abcam Cat# ab203491, RRID: AB_2892065) (Du et al. 2020), MBP (1:100 0, Abcam Cat# ab40390, RRID: AB_1141521) (Morrison et al. 2016), Sox10 (1:500, Abcam Cat# ab27655, RRID: AB_778021) (Falcone et al. 2019) and NKX2.2 (1:1000, TFS Cat# PA5-78079, RRID: AB_2736230). After 3 washes with TBS containing 0.1% Tween-20, the membranes were incubated at room temperature for 2 h with a horseradish peroxidase-conjugated goat anti-rabbit secondary antibody (1:5000, Abcam Cat# ab150077, RRID: AB_2630356). The bands of protein on the membranes were tested using a chemiluminescent substrate (1812401, Millipore, USA). The optical density of the protein bands was measured by ImageJ software (NIH, USA).

Transmission electron microscopy

Mice were sacrificed with an overdose of pentobarbital and perfused transcardially with fixative solution (2% paraformaldehyde, 2.5% glutaraldehyde in 0.1 M phosphate buffer, pH 7.4). Brains were quickly removed from the skull, and 3 mm-thick slabs containing the whole hippocampus were cut. The hippocampal tissues were immersed in the same fixative solution overnight at 4 °C. After rinsing in phosphate buffer, the tissues were postfixed in 1% osmium tetroxide (419494, Sigma-Aldrich) for 1 h and dehydrated in a series of graded acetone solutions. The specimens were embedded and cut with an ultramicrotome (DuPont-Sorvall, USA), stained with uranyl acetate and lead salts, and then observed under a transmission electron microscope (JEOL, Japan). Myelin in the CA1 region was assessed at 10000 magnification. The structure of myelin in the CA1 region was analyzed based on at least 20 images per animal that contained more than 200 axons. The g-ratio (inner axonal diameter to total outer diameter including myelin) was measured on the same myelin axonal structures as previously described (Chomiak et al. 2009).

Compound action potential (CAP) recording

The optic nerves of mice were dissected and incubated with oxygenated recording solution (in mM) at room temperature as follows: 125 NaCl, 2.5 KCl, 1 $MgCl_2$, 2 $CaCl_2$, 10 D-glucose, 1.25 NaH_2PO_4, and 25 $NaHCO_3$. After transfer to the recording chamber and visualization under a light microscope (Nikon, Japan), the ends of the optic nerves were suctioned into separate fire-polished borosilicate glass suction electrodes using 2 ml precision syringes (Gilmont, USA). A grid with 1 mm spacing was used to measure the nerve length. Constant current stimulation (50 s) was delivered to one end of the nerve using a stimulus isolator (ISO-Flex, Israel). Electrical signals were acquired using a differential AC amplifier (model 1700, AM Systems) and digitized using a digitizer (Axon Digidata 1440A, Molecular Devices). The recording chamber was constantly perfused with oxygenated recording solution delivered by gravity and removed via a peristaltic pump. Recordings of CAPs were taken by stimulating the nerve at one end and measuring the response at the other end. Conduction velocity was calculated by dividing the length of the nerve by the latency between the start of the stimulus artifact and the peak of the CAP. The normalized

half-width was determined by measuring the latency between the half-amplitude preceding and half-amplitude following the peak of the CAP and dividing it by the length of the nerve.

Behavioral analysis

Behavioral experiments were performed at PND60. To allow habituation and reduce stress, mice were moved to the experimental room 48 h before the start of the experiment (the brightness of the experimental room was 70 lux). Each experimental apparatus was cleaned with 75% ethanol after being exposed to a mouse to remove odor cues.

Novel object recognition (NOR). Two objects, which were different in shape and color but similar in size, were placed in an activity chamber. Each mouse was allowed to explore the chamber and objects for 10 min of training. Then, the mouse was moved to its home cage, and the chamber and objects were cleaned with ethanol to remove odor cues. One hour later, the mouse was allowed to explore the chamber and objects again for 5 min, with a novel object replacing one of the objects used in the training session. Discrimination scores were calculated by subtracting the number of nose pokes of the familiar object from the number of nose pokes of the novel object and dividing the difference by the total number of nose pokes of both objects.

Morris water maze (MWM). The water maze (diameter: 150 cm; height: 60 cm) was located in an isolated room and surrounded by a black curtain with four quadrants. Water (25 °C) was filled to the level of 1 cm over the platform. A video recording device connected to a computer with Any-Maze tracking software (Stoelting, USA) was used to track the movement of mice during swimming. For training, each mouse was given 60 s to locate the platform using the spatial cues in the room, after which the animal remained on the platform for 15 s (mice that could not find the platform within 60 s were guided to the platform for learning). Mice were trained by performing four trials daily for 4 days. On the fifth day, mice were allowed to swim freely in the maze, and the total time they spent in the platform quadrant and the crossing time were recorded.

Accelerating rotarod (AR). Motor function was tested using an accelerating rotarod (4–40 rpm, in 5 min; model 7650, Ugo Basile Biological Research Apparatus, Italy). Mice performed two trials per day with a 45~60-min intertrial interval for 5 consecutive days (at the same hour every day). For each day, the average time spent on the rotarod, or the time the mouse successfully made 3 consecutive wrapping/passive rotations (latency in seconds), was calculated. The maximum duration of a trial was 5 min.

Statistical analysis

GraphPad Prism 7.00 (GraphPad Software, USA) was used for statistical analysis. Analyses were performed in a manner where the person conducting the analyses was blinded to treatment assignments in all experiments. All data are expressed as the mean ± standard deviation (SD). Comparisons between two groups were performed using an unpaired *t*-test, Comparisons between multiple groups were

performed using a one-way ANOVA followed by Tukey-Kramer's *post hoc* test. Comparisons between multiple groups at different time point were performed using a two-way ANOVA followed by *post hoc* Bonferroni's test. $P < 0.05$ was considered to be statistically significant.

Results

Maternal exposure to sevoflurane causes cognitive and motor impairments in offspring

Pregnant mice (G15.5) received 2.5% sevoflurane for 6 h. The NOT test and the MWM test were conducted in the offspring at PND60 to assess their cognition, and the AR test was conducted to assess their motor coordination (Fig. 1a). In the NOR test, compared with control mice, sevoflurane-treated mice spent more time exploring the familiar object than the novel object (Fig. 1b-c). In the MWM test, the escape latency to reach the platform of sevoflurane-treated mice was significantly increased compared with that of the control mice during both training (Fig. d-e) and probe phases (Fig. f). We also observed that time spent in the target quadrant was substantially shorter in the sevoflurane-treated group than that in the control group (Fig. 1g), while total distance (Fig. 1h) and average speed (Fig. 1i) were not changed between two groups. In the AR test, mice in the sevoflurane-treated group showed a significant decrease in the latency to fall off the rotarod (Fig. 1j-k). Taken together, these results suggested that maternal exposure to sevoflurane induced impairments of cognitive and motor functions in developing offspring.

Suppressed OPC proliferation and differentiation after sevoflurane exposure

Primary cultured OPCs were treated with 4.1% sevoflurane for 6 h. BrdU incorporation and immunocytochemistry were performed to assess proliferation and differentiation of OPCs, respectively. For proliferation, the number of BrdU/Olig2 double-labeled cells was significantly decreased after sevoflurane exposure compared with that of the control group (Fig. 2a-b). For differentiation, the number of MBP/Olig2 double-labeled cells was also decreased (Fig. 2c-d). These results suggested that sevoflurane exposure caused inhibitions of proliferation and differentiation in cultured OPCs.

Damages of myelin structure in the postnatal hippocampus after maternal exposure to sevoflurane

To explore the effect of prenatal sevoflurane exposure on architecture of myelin in the hippocampus, we stained MBP at PND14, PND30 and PND60 after maternal exposure to sevoflurane. The results showed that myelinated fibers traversed throughout the stratum lacunosum-moleculare (SLM) and hilus in the hippocampus either in small groups or in individual strands (Fig. 3a). At PND14, the intensity of MBP immunoreactivity was significantly decreased in the CA2/CA3 regions after sevoflurane treatment. The intensity of MBP immunoreactivity showed decreasing trends in the CA1 and DG regions, but there were no significant differences (Fig. 3a-b). At PND30 and PND60, the intensity of MBP immunoreactivity in the whole hippocampus was significantly reduced, including CA1, CA2/CA3 and DG regions (Fig. 3a, c-d). These results demonstrated that prenatal exposure to sevoflurane caused damage to myelinated fibers during development of the hippocampus.

Next, transmission electron microscopy was utilized to evaluate ultrastructure of myelin after maternal exposure to sevoflurane. The results showed that at PND30 and PND60, the numbers of myelinated axons with compact layers in the sevoflurane group were significantly reduced compared with those in the control group (Fig. 3e). In addition, g-ratio was used as an index to assess structure and function of axonal myelin, as myelin sheaths thinner or thicker than the theoretical optimal g-ratio of 0.77 cause a decline in conduction velocity in the CNS (Chomiak et al. 2009; Hunt et al. 2017). We found that prenatal exposure to sevoflurane caused a significant increase in the g-ratio in the hippocampus compared with that of the control group at PND30 and PND60 (Fig. 3f, g). These results suggested that prenatal exposure to sevoflurane caused loosening of the myelin sheath in the hippocampus of the mouse brain.

Maternal exposure to sevoflurane reduces the expression of myelin-associated genes and proteins

To systematically evaluate the effects of prenatal exposure to sevoflurane on myelination of oligodendrocytes, we detected myelin-associated genes and proteins via immunofluorescence, western blotting and qRT-PCR. We found that maternal exposure to sevoflurane significantly reduced the expression of the $PDGFR\alpha^+$ oligodendrocyte precursor at PND30 (Fig. 4a-b). Colocalization of CC1 and Olig2 was conducted to assess the maturation of oligodendrocytes, and the number of $CC1^+/Olig2^+$ cells in the CA2/CA3 region at PND30 was reduced after sevoflurane treatment, but there were no significant changes in the CA1 and DG regions (Fig. 4c-d). We further confirmed probable changes in myelin morphology by calculating the distribution and contents of MBP and NF200 in the hilus region of DG. Immunofluorescence showed that the intensity of $MBP^+/NF200^+$ cells was significantly reduced in the sevoflurane-treated group at PND30 and PND60 compared with that in the control group (Fig. 4e-f), revealing an indirect effect of prenatal exposure to sevoflurane on myelination of postnatal hippocampus.

The mRNA and protein levels of myelination-regulating genes/transcription factors in the hippocampus were also detected, including Olig1, Olig2, Sox10, MBP, CNPase, myelin associated glycoprotein (MAG), myelin oligodendrocyte glycoprotein (MOG), chondroitin sulfate proteoglycan (NG2), myelin gene regulatory factor (MYRF), PDGFRα, and proteio lipid protein (PLP). qRT-PCR showed that almost all of these transcription factors were downregulated after sevoflurane treatment at PND30 and PND60 (Fig. 5a). Western blotting showed that the protein levels of PDGFRα, Sox10, Olig1 and MBP were decreased at PND30 and PND60, while the levels of NKX2.2 and Olig2 were not significantly changed (Fig. 5b-g). In conclusion, the above results suggested that maternal exposure to sevoflurane inhibited the expression of genes and proteins involved in the regulation of myelination in offspring.

Maternal exposure to sevoflurane attenuates the conductivity of axons in optic nerves

To investigate whether maternal exposure to sevoflurane caused functional changes in axonal myelin, we recorded the CAPs, the sum of the firing action potentials from isolated optic nerves (Fig. 6a). We observed that sevoflurane exposure resulted in a 37% reduction in the conduction velocity compared with that of the control group (Fig. 6b). Furthermore, the half-width of the CAP response in sevoflurane-

exposed mouse nerves was 1.4 times as wide as that in control mice (Fig. 6c). These findings suggested that maternal exposure to sevoflurane decreased the conduction velocity of optic nerve fibers in offspring.

Discussion

Every year, millions of pregnant women suffer from nonobstetric surgeries with general anesthetic exposure (Kuczkowski 2006; Okeagu et al. 2020). Although the safety of anesthetic agents has been guaranteed, the adverse effects of anesthetics on the development of the fetus are of great concern (Xu et al.; Yu et al.). It has been widely accepted that prenatal exposure to sevoflurane can induce impairment of cognitive function in offspring (Kang et al. 2017). However, studies of the effects of anesthesia-induced neurotoxicity have mainly focused on neurons, not glial cells (Vutskits et al. 2016). Given the integrity and essential role of oligodendrocytes in the development and functional maintenance of mouse brain (Philips et al. 2017; Xin et al. 2020), the potential effects of sevoflurane exposure on oligodendrocytes should not be neglected. In this study, by evaluating myelin-associated morphological and functional indices, we provided evidences that gestational exposure to sevoflurane could result in disruptions in oligodendrocyte development and myelination in the hippocampus after birth. In addition, we observed impairments of cognitive and motor functions in adult offspring. Our data suggested that myelination of oligodendrocytes might be involved in neurodevelopmental toxicity induced by sevoflurane.

Previous studies have reported that exposing pregnant mice to sevoflurane leads to increased risks on cognition in offspring (Zuo et al. 2020a). Myelin plays important structural and functional roles in the development of the brain, and degradation of myelin is a key feature of neurological disorders involving cognitive dysfunction (Park et al. 2016). In sevoflurane-induced neurotoxicity, the involvement of myelin alterations has also been proposed (Zhang et al. 2019). Here, we focused on the effects of maternal exposure to sevoflurane on myelin produced by oligodendrocytes in the fetus. We found that exposure to 2.5% sevoflurane for 6 h induced damages in the structure of myelin and downregulations of myelin-associated genes and proteins, which was supported by other investigations (Zuo et al. 2020b). In functional study, sevoflurane exposure attenuated the conductivity of axons. We guess these disruptions of myelination contribute to the impairment of cognitive function induced by sevoflurane exposure, which is worthy of further exploration.

In the CNS, myelination is a highly specialized and tightly regulated process that involves the proliferation, migration, and differentiation of OPCs into myelin-generating cells during development and throughout adulthood (Tsai et al. 2019). Myelination in the hippocampal axons has been reported to profoundly affect learning and memory via regulation of information processing in neural circuits (Fields 2015), and demyelination in the hippocampus is involved in several neurodegenerative and neurological disorders, including multiple sclerosis, Alzheimer's disease, and schizophrenia (Duncan et al. 2016). Herein, we investigated the effects of sevoflurane exposure during the mid-gestational period on hippocampal myelination. We found that sevoflurane exposure significantly decreased the number of

$BrdU^+/Olig2^+$ and $MBP^+/Olig2^+$ double-labeled cells *in vitro*, revealing inhibitions of OPC proliferation and differentiation. MBP is one of the most abundant structural proteins in myelin and can reflect myelinization and compaction in neuronal cells (Zuo et al. 2020b). We examined the formation and development of myelin sheaths in the hippocampus by studying the immunoreactivity of MBP *in vivo*. Significant reductions of the numbers of myelin fibers in the CA1, CA2/CA3 and DG regions at PND14, PND30 and PND60 were observed, and the g-ratio of the myelin sheath was markedly increased. Our findings indicated that prenatal exposure to sevoflurane induced deficits in myelin development.

We further confirm the effects of sevoflurane exposure on genes and proteins involved in the regulation of the myelination process via immunofluorescence, western blot analysis and qRT-PCR. We found that the levels of MBP, PLP, CNPase, PDGFRα, Olig1, Sox10, NKX2.2, and MYRF were downregulated in the sevoflurane-treated group compared with those in the control group at PND30 and PND60. Accordingly, MYRF plays an important role in oligodendrocyte differentiation and myelination (Aprato et al. 2020), and genes such as MAG, PLP, and MBP are downregulated after ablation of MYRF (Zhang et al. 2021). Thus, we speculated that the reductions in these genes might be due to decreased expression of MYRF following sevoflurane exposure. PLP is the second most abundant protein after MBP in the CNS and is involved in generating the multilayered structure of myelin. Neurotoxicants such as ethanol can reduce the expression of PLP and alter myelination in the hippocampus (Pascual et al. 2017). In addition, the reduced levels of CNPase induced by sevoflurane exposure found in our study might have led to reduced initiation of myelination, as observed in earlier studies (Dai et al. 2015). Our results suggested that prenatal exposure to sevoflurane suppressed myelination in multiple stages of development.

It is well established that myelin acts as an electrical insulator and facilitates the conduction of nerve impulses in axons, and a g-ratio of 0.77 is considered the structural and functional index of optimal axonal myelination (Chomiak et al. 2009; Dean et al. 2016). Sevoflurane exposure greatly attenuated the conductivity of axons. This might be due to loosening of the myelin sheath, as the g-ratio markedly increased after sevoflurane exposure. Adhesion molecules such as PLP, MAG, and MBP were decreased in our study. Thus, disruption of protein structural bonds between myelin layers may be responsible for the loosening of the myelin sheath, which has been reported in oxidative stress (Dąbrowska-Bouta et al. 2019; Ravera et al. 2015). Sevoflurane exposure may lead to the loss of cell adhesion molecules and myelin decompaction via lipid peroxidation. Further studies are needed to explore the exact cellular and molecular mechanisms involved in the effects of sevoflurane on the stability of the myelin sheath.

In conclusion, our results suggested that gestational exposure to sevoflurane had detrimental effects on oligodendrocyte development and axonal myelination in the hippocampus, which might be associated with sevoflurane-induced cognitive and motor abnormalities. Further studies should be conducted to clarify the exact mechanisms of these effects and offer a promising strategy for the treatment of sevoflurane-induced neurotoxicity.

Declarations

Author Contributions

Xianghui Zhao and Hui Zhang designed the experiments. Ze Fan, Lirong Liang, Ruixue Ma, Rougang Xie, Youyi Zhao and Ming Zhang performed the experiments. Danyi He, Tian Zeng and Baolin Guo interpreted the data and prepared the figures. Ze Fan Xianghui Zhao and Hui Zhang wrote and revised the manuscript.

Conflict of interest

The authors declare that this research was conducted without any commercial or financial relationships and that no conflict of interest exists.

Acknowledgements:

This study was supported by the Natural Science Foundation of China (No.81971076 and No. 81371265 to Hui Zhang), Science Innovation Promoting Program of Shaanxi Province (No.2014KTCL0305 to Hui Zhang), Natural Science of Shaanxi Province (No.2021JQ345 to Lirong Liang) and Assistance Program of the Third Affiliated Hospital of Fourth Military Medical University (No.2020QNYC05 to Ze Fan).

References

1. Andropoulos DB, Greene MF (2017) Anesthesia and Developing Brains - Implications of the FDA Warning. N Engl J Med 376(10):905–907
2. Aprato J, Sock E, Weider M, Elsesser O, Fröb F, Wegner M (2020) Myrf guides target gene selection of transcription factor Sox10 during oligodendroglial development. Nucleic acids research 48(3):1254–1270
3. Armistead J, Hatzold J, van Roye A, Fahle E, Hammerschmidt M (2020) Entosis and apical cell extrusion constitute a tumor-suppressive mechanism downstream of Matriptase. J Cell Biol 219(2):e201905190
4. Chai D, Cheng Y, Jiang H (2019) Fundamentals of fetal toxicity relevant to sevoflurane exposures during pregnancy. Int J Dev Neurosci 72:31–35
5. Chomiak T, Hu B (2009) What is the optimal value of the g-ratio for myelinated fibers in the rat CNS? A theoretical approach. PloS one 4(11):e7754
6. Cortés-Medina L, Pasantes-Morales H, Aguilera-Castrejon A, Picones A, Lara-Figueroa C, Luis E et al (2019) Neuronal Transdifferentiation Potential of Human Mesenchymal Stem Cells from Neonatal and Adult Sources by a Small Molecule Cocktail. Stem Cells International 2019:7627148
7. Dąbrowska-Bouta B, Sulkowski G, Strużyński W, Strużyńska L (2019) Prolonged Exposure to Silver Nanoparticles Results in Oxidative Stress in Cerebral Myelin. Neurotox Res 35(3):495–504
8. Dai J, Bercury KK, Ahrendsen JT, Macklin WB (2015) Olig1 function is required for oligodendrocyte differentiation in the mouse brain. The Journal of neuroscience: the official journal of the Society for Neuroscience 35(10):4386–4402

9. Dean D, O'Muircheartaigh J, Dirks H, Travers B, Adluru N, Alexander A et al (2016) Mapping an index of the myelin g-ratio in infants using magnetic resonance imaging. NeuroImage 132:225–237
10. Dong C, Rovnaghi CR, Anand KJ (2016) Ketamine exposure during embryogenesis inhibits cellular proliferation in rat fetal cortical neurogenic regions. Acta anaesthesiologica Scandinavica 60(5):579–587
11. Du Z, Yin S, Song X, Zhang L, Yue S, Jia X et al (2020) Identification of Differentially Expressed Genes and Key Pathways in the Dorsal Root Ganglion After Chronic Compression. Frontiers in Molecluar Neuroscience 13:71
12. Duncan ID, Radcliff AB (2016) Inherited and acquired disorders of myelin: The underlying myelin pathology. Exp Neurol 283:452–475
13. Elbaz B, Popko B (2019) Molecular Control of Oligodendrocyte Development. Trends in neurosciences 42(4):263–277
14. Falcone C, Wolf-Ochoa M, Amina S, Hong T, Vakilzadeh G, Hopkins W et al (2019) Cortical interlaminar astrocytes across the therian mammal radiation. Journal of Comparative Neurology 527(10):1654–1674
15. Fang F, Song R, Ling X, Peng M, Xue Z, Cang J (2017) Multiple sevoflurane anesthesia in pregnant mice inhibits neurogenesis of fetal hippocampus via repressing transcription factor Pax6. Life sciences 175:16–22
16. Fields R (2015) A new mechanism of nervous system plasticity: activity-dependent myelination. Nature reviews Neuroscience 16(12):756–767
17. Göttle P, Sabo J, Heinen A, Venables G, Torres K, Tzekova N et al (2015) Oligodendroglial maturation is dependent on intracellular protein shuttling. J Neurosci 35(3):906–919
18. Hunt M, Lu P, Tuszynski M (2017) Myelination of axons emerging from neural progenitor grafts after spinal cord injury. Exp Neurol 296:69–73
19. Ishii A, Furusho M, Macklin W, Bansal R (2019) Independent and cooperative roles of the Mek/ERK1/2-MAPK and PI3K/Akt/mTOR pathways during developmental myelination and in adulthood. Gia 67(7):1277–1295
20. Kang E, Jiang D, Ryu YK, Lim S, Kwak M, Gray CD et al (2017) Early postnatal exposure to isoflurane causes cognitive deficits and disrupts development of newborn hippocampal neurons via activation of the mTOR pathway. PLoS Biol 15(7):e2001246
21. Kuczkowski K (2006) The safety of anaesthetics in pregnant women. Exp Opin Drug Saf 5(2):251–264
22. Lee S, Chung W, Park H, Park H, Yoon S, Park S et al (2017) Single and multiple sevoflurane exposures during pregnancy and offspring behavior in mice. Paediatric anaesthesia 27(7):742–751
23. Li B, Liang F, Ding X, Yan Q, Zhao Y, Zhang X et al (2019) Interval and continuous exercise overcome memory deficits related to β-Amyloid accumulation through modulating mitochondrial dynamics. Behav Brain Res 376:112171

24. Lu W, Yang S, Zhang L, Chen L, Chao FL, Luo YM et al (2016) Decreased Myelinated Fibers in the Hippocampal Dentate Gyrus of the Tg2576 Mouse Model of Alzheimer's Disease. Curr Alzheimer Res 13(9):1040–1047
25. Makaryus R, Lee H, Feng T, Park JH, Nedergaard M, Jacob Z et al (2015) Brain maturation in neonatal rodents is impeded by sevoflurane anesthesia. Anesthesiology 123(3):557–568
26. Milosevic A, Liebmann T, Knudsen M, Schintu N, Svenningsson P, Greengard PJTJocn (2017) Cell- and region-specific expression of depression-related protein p11 (S100a10) in the brain. Journal of Comparative Neurology 525(4):955–975
27. Morrison K, Narasimhan S, Fein E, Bale TJE (2016) Peripubertal Stress With Social Support Promotes Resilience in the Face of Aging. Endocrinology 157(5):2002–2014
28. Neag MA, Mitre AO, Catinean A, Mitre CI (2020) An Overview on the Mechanisms of Neuroprotection and Neurotoxicity of Isoflurane and Sevoflurane in Experimental Studies. Brain research bulletin 165:281–289
29. Okeagu C, Anandi P, Gennuso S, Hyatali F, Stark C, Prabhakar A et al (2020) Clinical management of the pregnant patient undergoing non-obstetric surgery: Review of guidelines. Best practice research Clinical anaesthesiology 34(2):269–281
30. Park J, Choi H, Cho J, Kim I, Lee T, Lee J et al (2016) Effects of Chronic Scopolamine Treatment on Cognitive Impairments and Myelin Basic Protein Expression in the Mouse Hippocampus. Journal of molecular neuroscience: MN 59(4):579–589
31. Pascual M, Montesinos J, Montagud-Romero S, Forteza J, Rodríguez-Arias M, Miñarro J et al (2017) TLR4 response mediates ethanol-induced neurodevelopment alterations in a model of fetal alcohol spectrum disorders. J Neuroinflamm 14(1):145
32. Perez-Zoghbi JF, Zhu W, Grafe MR, Brambrink AM (2017) Dexmedetomidine-mediated neuroprotection against sevoflurane-induced neurotoxicity extends to several brain regions in neonatal rats. Br J Anaesth 119(3):506–516
33. Philips T, Rothstein J (2017) Oligodendroglia: metabolic supporters of neurons. J Clin Investig 127(9):3271–3280
34. Ravera S, Bartolucci M, Cuccarolo P, Litamè E, Illarcio M, Calzia D et al (2015) Oxidative stress in myelin sheath: The other face of the extramitochondrial oxidative phosphorylation ability. Free Radic Res 49(9):1156–1164
35. Tsai E, Casaccia P (2019) Mechano-modulation of nuclear events regulating oligodendrocyte progenitor gene expression. Glia 67(7):1229–1239
36. Vutskits L, Xie Z (2016) Lasting impact of general anaesthesia on the brain: mechanisms and relevance. Nature reviews Neuroscience 17(11):705–717
37. Wang Y, Yin S, Xue H, Yang Y, Zhang N, Zhao P (2018) Mid-gestational sevoflurane exposure inhibits fetal neural stem cell proliferation and impairs postnatal learning and memory function in a dose-dependent manner. Developmental biology 435(2):185–197

38. Wong FK, Fei JF, Mora-Bermúdez F, Taverna E, Haffner C, Fu J et al (2015) Sustained Pax6 Expression Generates Primate-like Basal Radial Glia in Developing Mouse Neocortex. PLoS Biol 13(8):e1002217
39. Wu Z, Li X, Zhang Y, Tong D, Wang L, Zhao P (2018) Effects of Sevoflurane Exposure During Mid-Pregnancy on Learning and Memory in Offspring Rats: Beneficial Effects of Maternal Exercise. Frontiers in cellular neuroscience 12:122
40. Xin W, Chan J (2020) Myelin plasticity: sculpting circuits in learning and memory. Nature reviews Neuroscience 21(12):682–694
41. Xu L, Shen J, Yu L, Sun J, McQuillan PM, Hu Z et al (2018) Role of autophagy in sevoflurane-induced neurotoxicity in neonatal rat hippocampal cells. Brain research bulletin 140:291–298
42. Xu RA-O, Zhu YA-O, Jia JA-O, Li WA-O, Lu YA-O (2021) RIPK1/RIPK3-Mediated Necroptosis is Involved in Sevoflurane-Induced Neonatal Neurotoxicity in the Rat Hippocampus. Cell Mol Neurobiol. doi:10.1007/s10571-021-01098-z
43. Yu Z, Wang J, Wang HA-O, Wang J, Cui J, Junzhang P (2020) Effects of Sevoflurane Exposure During Late Pregnancy on Brain Development and Beneficial Effects of Enriched Environment on Offspring Cognition. Cell Mol Neurobiol 40(8):1339–1352
44. Zhang L, Xue Z, Liu Q, Liu Y, Xi S, Cheng Y et al (2019) Disrupted folate metabolism with anesthesia leads to myelination deficits mediated by epigenetic regulation of ERMN. EBioMedicine 43:473–486
45. Zhang Z, Wang J, Song Z, Wang Y, Cheng Z, Guo Q et al (2021) Downregulation of microRNA-199a-5p alleviated lidocaine-induced sensory dysfunction and spinal cord myelin lesions in a rat model. Toxicology letters 336:1–10
46. Zheng H, Dong Y, Xu Z, Crosby G, Culley D, Zhang Y et al (2013) Sevoflurane anesthesia in pregnant mice induces neurotoxicity in fetal and offspring mice. Anesthesiology 118(3):516–526
47. Zuo Y, Chang Y, Thirupathi A, Zhou C, Shi Z (2020a) Prenatal sevoflurane exposure: Effects of iron metabolic dysfunction on offspring cognition and potential mechanism. International journal of developmental neuroscience: the official journal of the International Society for Developmental Neuroscience 81(1):1–9
48. Zuo Y, Li B, Xie J, Ma Z, Thirupathi A, Yu P et al (2020b) Sevoflurane anesthesia during pregnancy in mice induces cognitive impairment in the offspring by causing iron deficiency and inhibiting myelinogenesis. Neurochem Int 135:104693

Figures

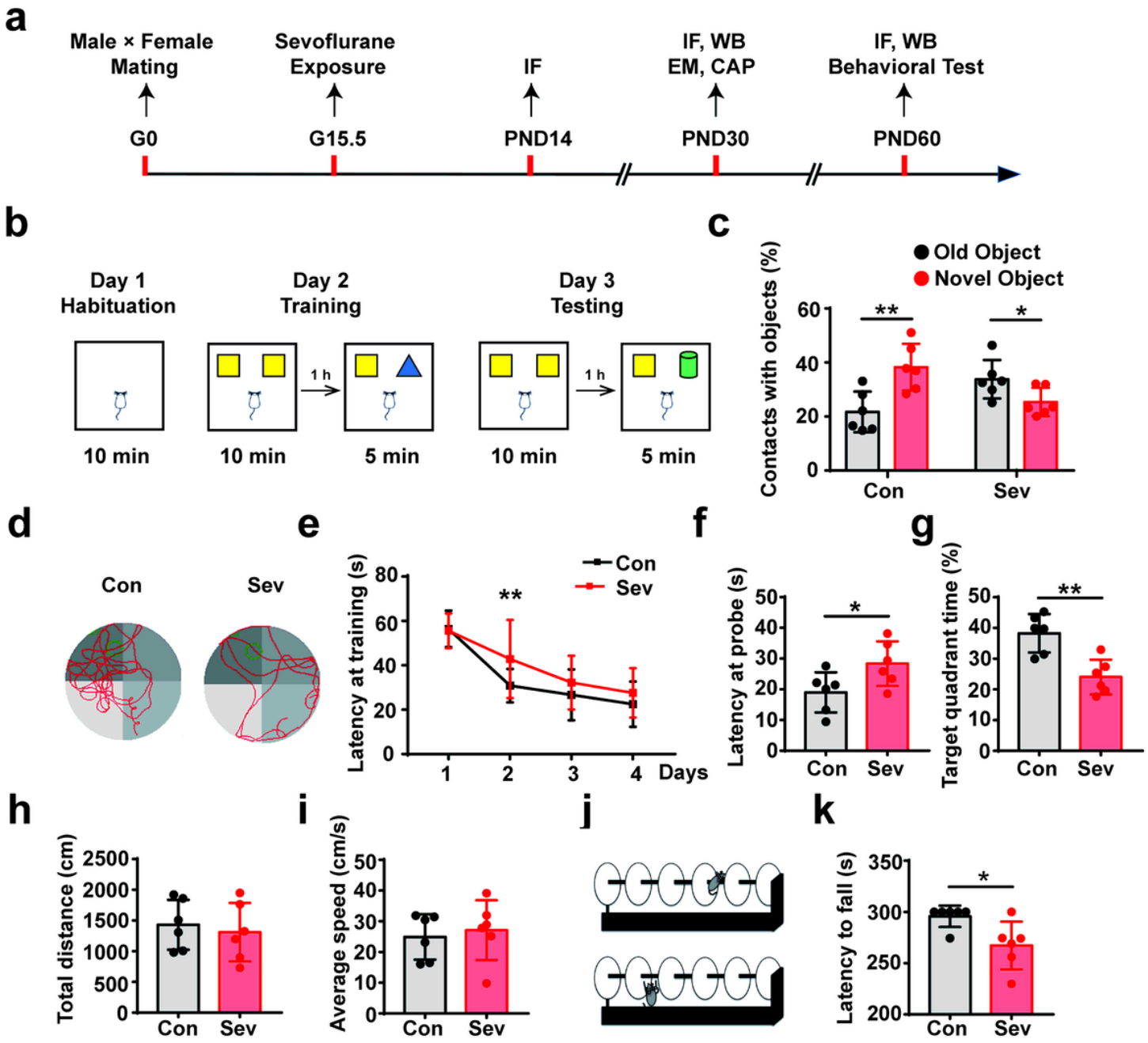

Figure 1

Gestational exposure to sevoflurane induces cognition and motor coordination impairments in offspring at PND60 (a) Schematic diagram for the time course of sevoflurane exposure and the assays. (b) Patterns of the novel object recognition test. (c) Proportions of contacts with novel and familiar objects of control and sevoflurane-treated mice (n=6 per group, *p < 0.05, **p < 0.01). (d) Typical diagrams of swimming in the Morris water maze test. (e) Latency to platform of the mice during days 1-4 in the Morris water maze test (n=6 per group, **p < 0.01). (f) Latency to platform of the mice at probe in the Morris water maze test (n=6 per group, *p < 0.05). (g) Relative time spent in the target quadrant platform (n=6 per group, **p < 0.01). (h) Total distance and (i) average speed of the mice in the Morris water maze test. (j) Schematic diagram of the accelerating rotarod test. (k) Latency to falling off the rotarod in the accelerating rotarod test (n=6 per group, *p < 0.05).

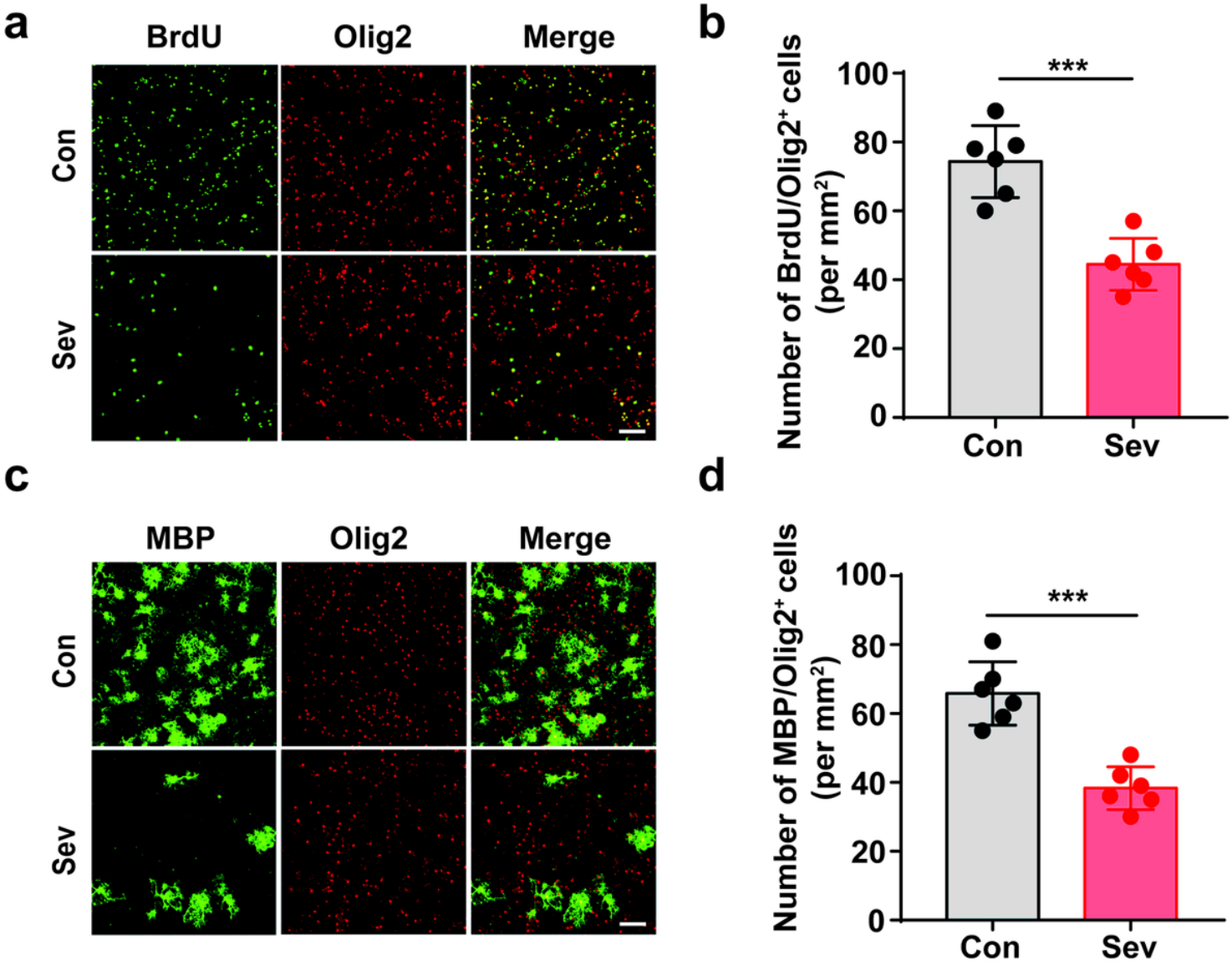

Figure 2

Sevoflurane inhibits the proliferation and differentiation of hippocampal-derived OPCs in vitro (a) Representative images of BrdU/Olig2 colocalization. Scale bar=100 μm. (b) BrdU (green) colocalized with Olig2 (red) was decreased in the sevoflurane-exposed groups compared with that in the control group (n=6 per group, ***p<0.001). (c) Representative images of MBP/Olig2 colocalization. Scale bar=100 μm. (d) MBP (green) colocalized with Olig2 (red) was decreased in the sevoflurane-exposed groups compared with that in the control group (n=6 per group, ***p<0.001).

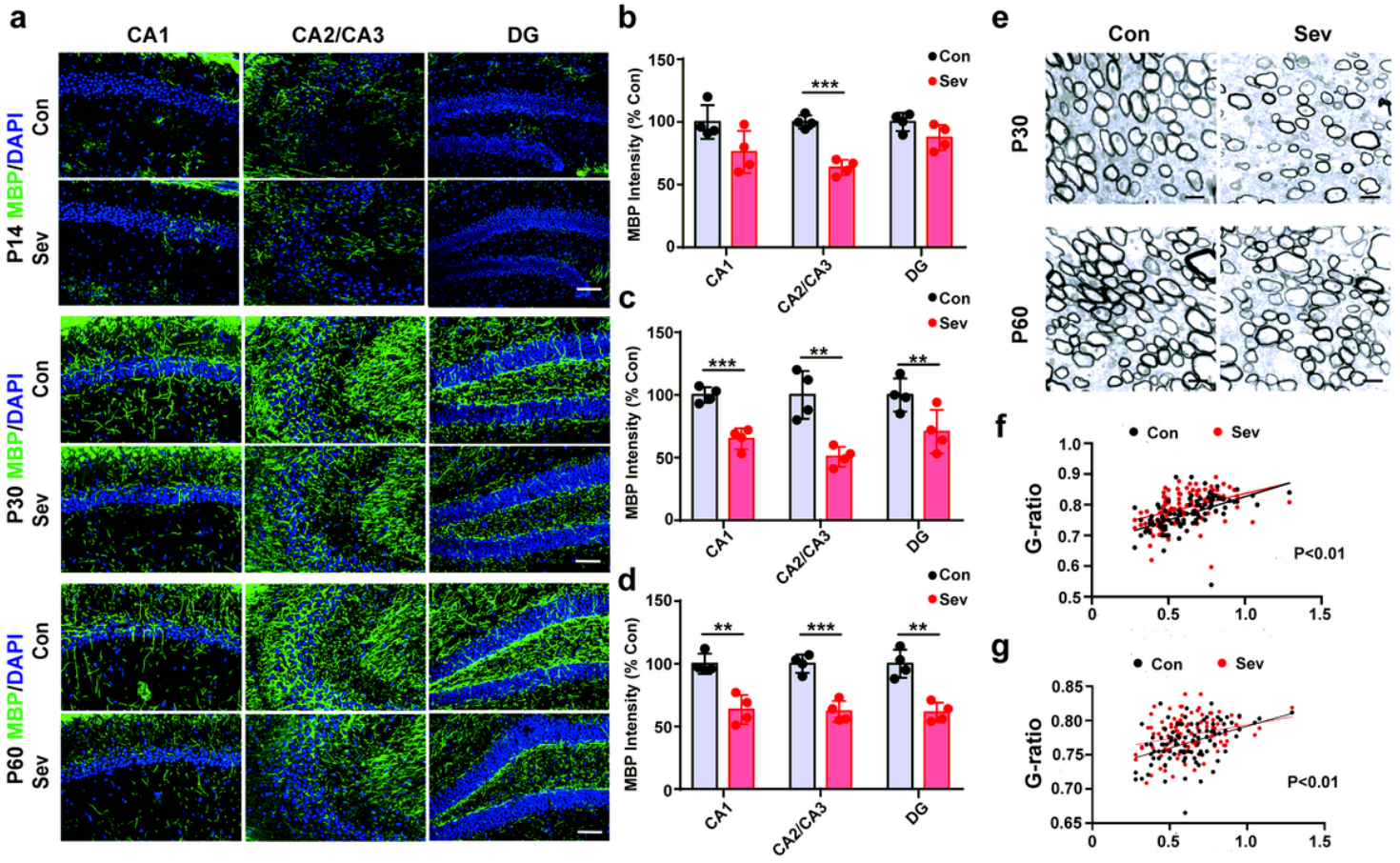

Figure 3

(a) Representative images showing the immunoreactivity of MBP+ fibers in the CA1, CA2/3 and DG regions of the hippocampus at different time points. Scale bar=100 μm. Graph showing the fluorescence intensity of MBP-positive fibers. (b) The MBP intensity in the CA2/3 regions was significantly reduced after sevoflurane exposure compared with that in the control group (n=4 per group, ***p<0.001). At (c) PND30 and (d) PND60, the MBP intensity in the whole hippocampus (including the CA1, CA2/CA3 and DG regions) was significantly reduced compared with that in the control group (n=4 per group, **p<0.01, ***p < 0.001). (e) Representative electron microscopic images of the ultrastructure of myelinated axons in the hippocampus of control and sevoflurane-treated mice at PND30 and PND60. Scale bar=100 nm. (f) Graphical representation of the axonal g-ratio at PND30 (n=6 per group, **p<0.01). (g) Graphical representation of the axonal g-ratio at PND60 (n=6 per group, **p<0.01). DG, dentate gyrus; CA, cornu ammonis.

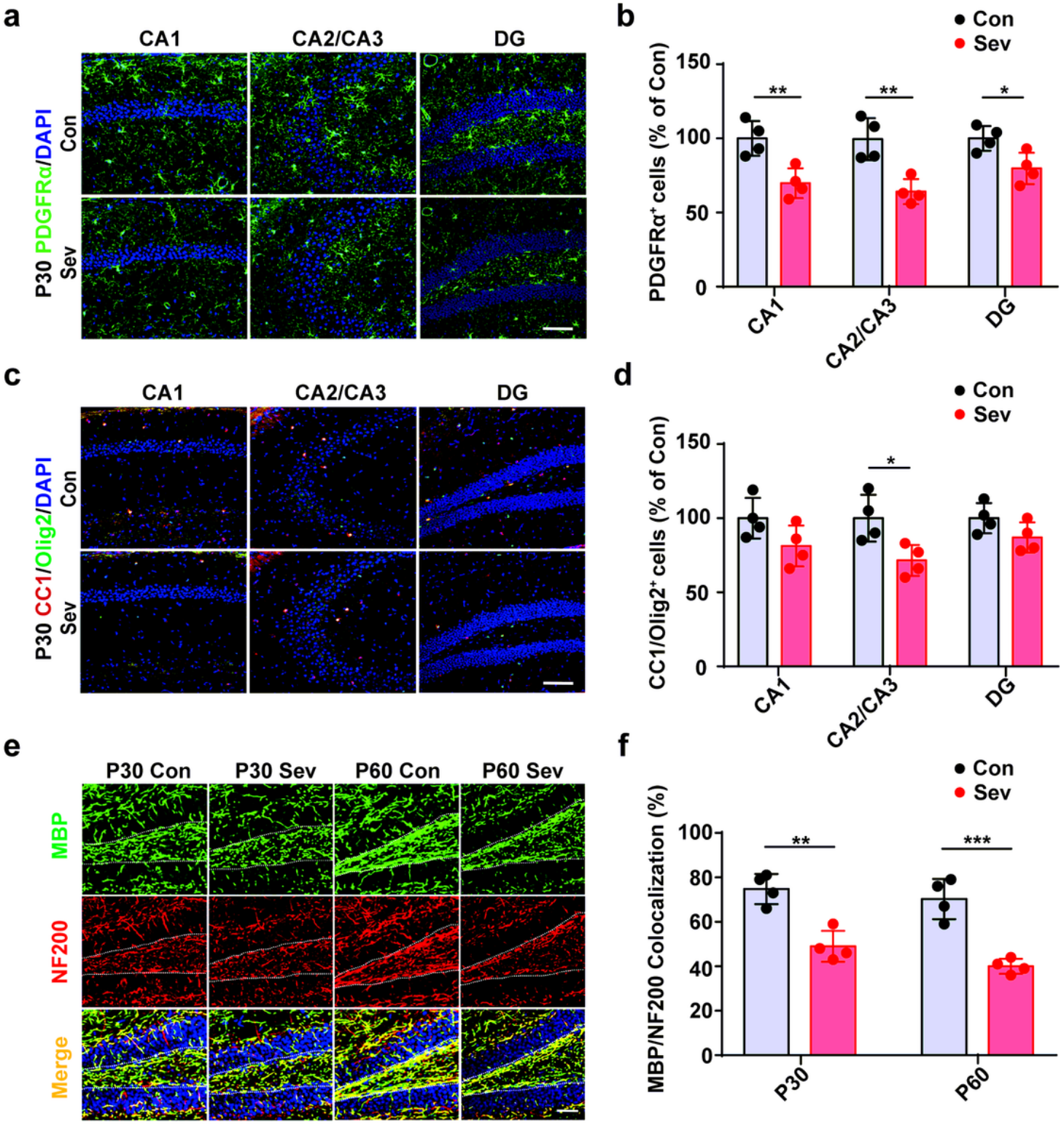

Figure 4

Immunofluorescence staining of myelin-associated proteins after prenatal exposure to sevoflurane (a) Immunoreactivity of PDGFRα in the CA1, CA2/3, and DG regions of the hippocampus at PND30. Scale bar=100 μm. (b) Relative quantitative analysis showing that the PDGFRα intensity in the CA1, CA2/3 and DG regions was significantly reduced after sevoflurane exposure compared with that in the control group (n=4 per group, *p<0.05, **p<0.01). (c) Colocalization of CC1/Olig2 in the CA1, CA2/3, and DG regions of

the hippocampus at PND30. Scale bar=100 μm. (d) Relative quantitative analysis showing that CC1+/Olig2+ cells in CA2/3 were significantly reduced after sevoflurane exposure compared with those in the control group (n=4 per group, *p<0.05). (e) Colocalization of MBP/NF200 in the DG region of the hippocampus at PND30 and PND60. Scale bar=100 μm. (f) Relative quantitative analysis showing that at PND30 and PND60, MBP+/NF200+ cells in the DG region were significantly reduced after sevoflurane exposure compared with those in the control group (n=4 per group, **p<0.01, ***p<0.001).

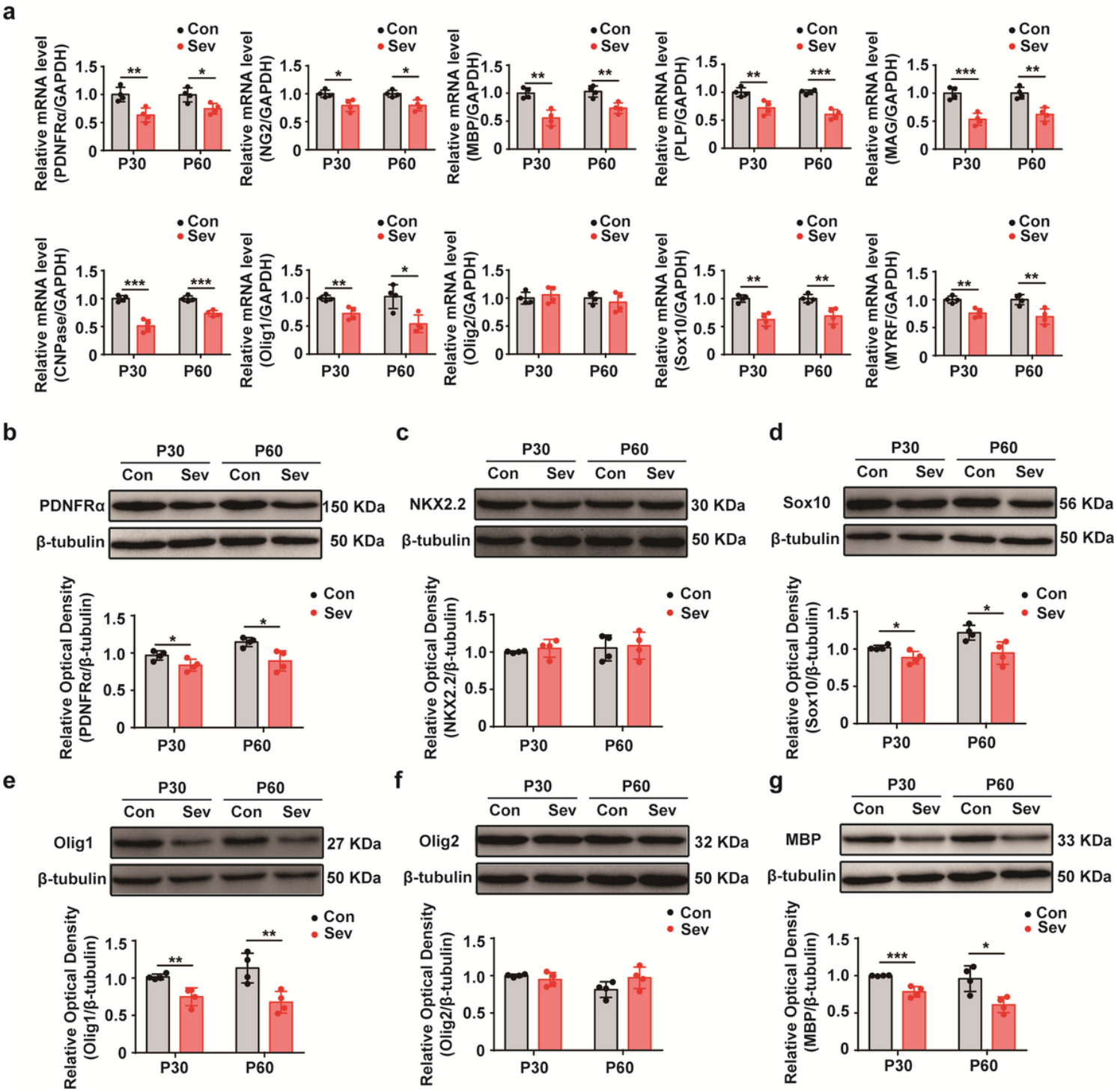

Figure 5

Levels of myelin-associated mRNAs and proteins after prenatal exposure to sevoflurane (a) Quantitative real-time PCR analysis of the relative mRNA expression of genes that are involved in myelination at PND30 and PND60. GAPDH served as the housekeeping gene for normalization. (n=4 per group, *p<0.05, **p<0.01, ***p<0.001). (b-e) Western blot analysis of the PDGFRα, NKX2.2, Sox10, Olig1, Olig2 and MBP protein levels in the hippocampus. The values were normalized to that of β-tubulin. (n=4 per group, *p<0.05, **p<0.01, ***p<0.001).

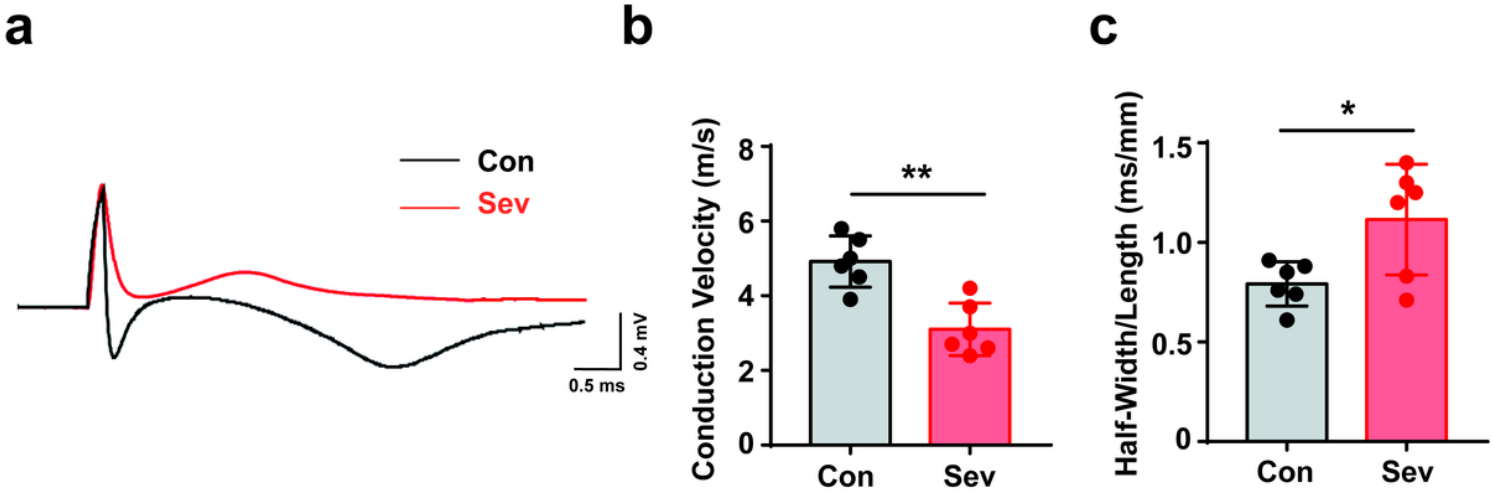

Figure 6

Alterations in axonal conductivity after prenatal exposure to sevoflurane (a) Representative traces of CAP recordings from isolated optic nerves of control (black) and sevoflurane-treated (red) mice. (b) Quantification of the conduction velocity of control and sevoflurane-treated nerves (n=6 per group, **p<0.01). (c) Half-width of the CAP response normalized to the length of the nerve (n=6 per group, *p<0.05).

Supplementary Files

This is a list of supplementary files associated with this preprint. Click to download.

- FullgelsWesternblot.docx